MOLECULAR IMAGING AND BIOLOGY

Mol Imaging Biol (2019) 21:122–129
DOI: 10.1007/s11307-018-1214-y

Published Online: 29 May 2018

RESEARCH ARTICLE

A Novel PET Probe "[^{18}F]DiFA" Accumulates in Hypoxic Region *via* Glutathione Conjugation Following Reductive Metabolism

Yoichi Shimizu,[1,2,3] Songji Zhao,[4] Hironobu Yasui,[2,4] Ken-ichi Nishijima,[2] Hiroki Matsumoto,[5] Tohru Shiga,[4] Nagara Tamaki,[4] Mikako Ogawa,[1] Yuji Kuge[2,4]

[1]*Laboratory of Bioanalysis and Molecular Imaging, Graduate School of Pharmaceutical Sciences, Hokkaido University, Kita 12, Nishi 6, Kita-ku, Sapporo, 060-0812, Japan*
[2]*Central Institute of Isotope Science, Hokkaido University, Kita 15 Nishi 7, Kita-ku, Sapporo, 060-0815, Japan*
[3]*Kyoto University Hospital, 54 Shogoinkawahara-cho, Sakyo-ku, Kyoto, 606-8507, Japan*
[4]*Graduate School of Medicine, Hokkaido University, Kita 15 Nishi 7, Kita-ku, Sapporo, 060-8638, Japan*
[5]*Research Centre, Nihon Medi-Physics Co., Ltd., 3-1 Kitatode, Sodegaura, Chiba, 299-0266, Japan*

Abstract

Purpose: Hypoxia in tumor has close relationship with angiogenesis and tumor progression. Previously, we developed 2,2-dihydroxymethyl-3-[^{18}F]fluoropropyl-2-nitroimidazole ([^{18}F]DiFA) as a novel positron emission tomography (PET) probe for diagnosis of hypoxia. In this study, we elucidated whether the accumulation of [^{18}F]DiFA in cells is dependent on the hypoxic state and revealed how [^{18}F]DiFA accumulates in hypoxic cells in combination with imaging mass spectrometry (IMS).

Procedures: FaDu human head and neck cancer cells were treated with [^{18}F]DiFA and then incubated under normoxia (21% O_2) or hypoxia (1% O_2) for 2 h. The cells were extracted using methanol, and the radioactivities of the precipitates (macromolecule fraction) and supernatants (low-molecular-weight fraction) were measured. FaDu-bearing mice were injected intravenously with [^{18}F]DiFA and with pimonidazole 1 h later. The tumors were excised 2 h after the injection of [^{18}F]DiFA. Autoradiography, IMS, and immunohistochemical (IHC) staining for pimonidazole were performed with serial tumor sections.

Results: In the *in vitro* study, the radioactivity of FaDu cells was significantly higher under hypoxia than that under normoxia (0.53 ± 0.02 *vs.* 0.27 ± 0.02 %dose/mg protein, $p < 0.05$). The radioactivity of the low-molecular-weight fraction was 66.3 ± 0.6% in the hypoxic cell. In the *in vivo* study, [^{18}F]DiFA accumulated in the tumor tissues existed mainly as low-molecular-weight compounds (90.4 ± 0.9%). In addition, the glutathione conjugate of reductive DiFA metabolite (amino-DiFA-GS) existed in tumor tissues revealed by the IMS study, and the distribution pattern of amino-DiFA-GS was very similar to that of the radioactivity and the positive staining area of pimonidazole.

Conclusions: Our results suggest that [^{18}F]DiFA undergoes the glutathione conjugation reaction following reductive metabolism in hypoxic cells, which leads hypoxia-specific PET imaging with [^{18}F]DiFA.

Key words: DiFA, Hypoxia, Imaging mass spectrometry, Molecular imaging, Glutathione

Electronic supplementary material The online version of this article (https://doi.org/10.1007/s11307-018-1214-y) contains supplementary material, which is available to authorized users.

Correspondence to: Yoichi Shimizu; *e-mail:* yoichis@kuhp.kyoto-u.ac.jp

Introduction

In solid tumor tissues, low oxygen concentration or hypoxia is known to play a pivotal role in tumor progression and angiogenesis. Hypoxia is associated with cancer resistance towards chemotherapy and radiotherapy [1, 2]. Thus, the precise detection of the hypoxic regions in tumor tissues provides valuable information for the improvement of cancer therapy.

To precisely identify the tumor hypoxic regions, various imaging modalities, especially positron emission tomography (PET), have been used [3, 4]. Radiolabeled 2-nitroimidazole-based compounds have been developed as PET imaging probes for hypoxia imaging [5, 6]. Among those agents, 1-(2-nitro-imidazolyl)-3-[^{18}F]fluoro-2-propanol ([^{18}F]FMISO) is the most widely used hypoxia-imaging probe in clinical diagnosis [7, 8]. [^{18}F]FMISO provides specific visualization of tumor hypoxic regions. However, it shows slow clearance from normal tissues owing to its lipophilicity, resulting in a high background level of [^{18}F]FMISO, and it takes a relatively long time to visualize hypoxic regions using this probe [9]. In a clinical trial, it took 4 hour to acquire highly reproducible images of hypoxic regions with [^{18}F]FMISO, which would burden patients [10]. To overcome this problem, our group has developed a novel hypoxia-imaging probe, 2,2-dihydroxymethyl-3-[^{18}F]fluoropropyl-2-nitroimidazole ([^{18}F]DiFA) (Fig. 1), which is more hydrophilic than [^{18}F]FMISO, and the preclinical and clinical studies of [^{18}F]DiFA are now in progress [11]. However, it still remains unclear whether [^{18}F]DiFA can really visualize cells depending on the hypoxic state, and how it accumulates in the hypoxic cells.

In this work, we first performed an *in vitro* study to elucidate whether [^{18}F]DiFA accumulates specifically in the hypoxic region. We then performed an *in vivo* study in combination with mass spectrometry, especially with imaging mass spectrometry (IMS), to reveal the mechanism of [^{18}F]DiFA accumulation in hypoxic cells.

Materials and Methods

Chemicals and Reagents

[^{18}F]DiFA was synthesized at the Hokkaido University Hospital Cyclotron Facility as previously described [11].

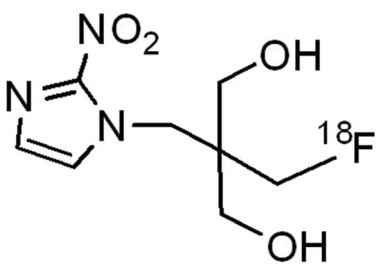

Fig. 1. Chemical structure of [^{18}F]DiFA.

Non-radiolabeled DiFA and amino-DiFA-GS were supplied by Nihon Medi-Physics Co., Ltd. Other chemicals were commercially available and of the highest available purity.

Cellular Uptake Study

FaDu human head and neck cancer cells (American Type Culture Collection, Manassas, VA, USA) were maintained in Eagle's minimum essential medium (Sigma–Aldrich, St. Louis, MO, USA), supplemented with 10% fetal bovine serum and penicillin (100 u/mL)–streptomycin (100 µg/mL) at 37 °C in a humidified atmosphere of 95% air and 5% CO_2 (normoxia). The cellular uptake study was performed in accordance with our previous work with some modification [12]. In brief, the cells were preincubated either under normoxia or under hypoxia with the oxygen levels at 1% *v*/*v* in an Invivo$_2$ 300 incubator (Baker Ruskinn, Ltd., Sanford, ME, USA) at 37 °C in a humidified atmosphere containing 5% CO_2 for 18 h. After preincubation, the cells were treated with [^{18}F]DiFA or [^{18}F]FMISO (2.5 MBq/well) and then were incubated under the same condition of the preincubation. After 2 h incubation, the cells were washed with phosphate-buffered saline (PBS) three times. After suspending the cells in methanol and centrifugation, the radioactivities of the supernatants and precipitates were measured with a Wizard 2480 Gamma Counter (PerkinElmer, Inc., Waltham, MA, USA). The supernatants and precipitates were considered as the low-molecular-weight and macromolecule-bound fractions, respectively. The precipitates were then lysed with 1 N NaOH, and the protein concentrations of the cell lysates were measured by the bicinchoninic acid (BCA) assay.

Tumor Xenograft Model

The protocols for the experiments with tumor xenograft model mice were approved by the Laboratory Animal Care and Use Committee of Hokkaido University. The animal experiments were performed in accordance with the Guidelines for Animal Experiments of the Graduate School of Medicine, Hokkaido University. The mice were housed under a 12-h light/12-h dark cycle with food and water supplied *ad libitum*. The tumor xenograft model mice were prepared by the previously reported method [13]. In brief, FaDu cells (5×10^6 cells/100 µL PBS) were inoculated into the right flank of BALB/c athymic nude mice (male, 9 weeks) (Japan SLC, Inc., Hamamatsu, Japan). The acquired tumor xenograft model mice were used for the animal study 2 weeks after the inoculation. All animal manipulations were performed by the sterile techniques.

Animal Experiments

[18F]DiFA (10 MBq) including non-radiolabeled DiFA (550 mg/kg body weight), in 25% dimethylacetamide solution, was intravenously injected into the FaDu-tumor-bearing mice. At 0.5 h (for the group euthanized at 1 h) or 1 h (for the group euthanized at 2 h) after the administration of [18F]DiFA, pimonidazole (100 mg/kg body weight; Hypoxyprobe Inc., Burlington, MA, USA) was administered into the same mice *via* the tail vein. At 1 or 2 h after the administration of [18F]DiFA, the mice were euthanized, and tumor, blood, heart, liver, kidney, muscle and bone were excised. The excised tissues were measured their weight and then were counted their radioactivities by a Wizard 2480 Gamma Counter (PerkinElmer, Inc.). The excised tumor tissues were cut into two pieces, and half of the tumor tissues were frozen by dry ice powder immediately. The serial cross sections were obtained with 10 μm thickness by a CM3050-Cryostat (Leica Microsystems, Wetzlar, Germany) and then were thaw-mounted on a glass slide. The other half of the tumor tissues were cut, frozen, and then homogenized in accordance with a previously reported method [13]. In brief, the frozen tumor tissues were suspended in PBS including a protease inhibitor (Roche Diagnostics, Basel, Switzerland) and then were pulverized with two types of zirconia beads with their diameter of 1 and 3 mm by vigorous vortex at 3000 rpm for 60 s using a Micro Smash™ instrument (Tomy Seiko Co., Ltd., Tokyo, Japan) at 4 °C. The tumor homogenates were then extracted with methanol twice, and the radioactivities in the supernatants and precipitates were measured by a Wizard 2480 Gamma Counter (PerkinElmer, Inc.). [18F]FMISO (10 MBq) with non-radiolabeled FMISO (550 mg/kg body weight) was also intravenously administered in FaDu-tumor-bearing mice, and the tumor tissues were excised 2 h after administration. The preparation of tumor homogenates and the measurement of radioactivities were performed by the same method shown above.

Autoradiography

The distribution of F-18 radioactivity in tumor tissues was observed by a previously reported autoradiography method [13]. In brief, the frozen tumor tissue sections were exposed to a BAS-SR phosphor-imaging plate (Fuji Photo Film Co., Ltd., Tokyo, Japan) overnight. Then, the autoradiogram images were obtained by a FLA 7000 Bio-Imaging Analyzer (Fuji Photo Film Co., Ltd.) and were analyzed by a Multi Gauge V3.2 software (Fuji Photo Film Co.).

Immunohistochemical Staining of Pimonidazole

Immunohistochemical staining of pimonidazole was performed to assess the hypoxic regions in tumor tissues by the method described previously [14]. In brief, the tissue sections were rehydrated and then were incubated with 0.3% hydrogen peroxide for 10 min to block endogenous peroxidase activity. The sections were treated with Hypoxyprobe-1 MAb1 antibody (Hypoxyprobe Inc.) for 30 min at 37 °C, followed by treatment with biotin-conjugated $F(ab')_2$ for 15 min at 37 °C. The sections were incubated with streptavidin and 3,3′-diaminobenzidine tetrahydrochloride to visualize the bound antibody complex on the sections. The stained images were obtained by a Biozero BZ-8000 microscope (Keyence Co., Osaka, Japan).

Matrix-Assisted Laser Desorption/Ionization-Imaging Mass Spectrometry Study

The preparation of the tissue section samples and the acquisition of matrix-assisted laser desorption/ionization-imaging mass spectrometry (MALDI-IMS) images were in accordance with our previous study with some modification [13, 14]. In brief, the acquired tumor sections were placed on indium tin oxide (ITO)-coated glass slides (Bruker Daltonics Inc., Billerica, MA, USA) and then stored at − 80 °C until analysis. The sections were dried with a vacuum desiccator over 15 min at room temperature, and the optical images were acquired using a scanner (GT-X820; Seiko Epson Corporation, Nagano, Japan). The matrix solution (30 mg/mL 2,5-dihydroxybenzoic acid dissolved in a 50% methanol solution containing 0.2% trifluoroacetic acid) was sprayed on the tissue sections by ImagePrep (Bruker Daltonics Inc.). The IMS study was performed with a 7-T Bruker solariX XR MALDI-Fourier transform-ion cyclotron resonance mass spectrometer (FT-ICR MS; Bruker Daltonics Inc.). Data were acquired in the positive-ion mode and with the laser energy and raster step size of 30–40% and 125 μm, respectively. The acquired data were analyzed using flexImaging 4.3 software (Bruker Daltonics Inc.). The obtained peak acquired on the tumor tissue sections was collected and split by collision-induced dissociation (CID) fragmentation to obtain structural information. The authentic amino-DiFA-GS placed on the ITO-coated glass and then coated with the matrix solution [30 mg/mL DHB dissolved in 1:1 (*v*/*v*) methanol–water containing 0.2% TFA] was also split by CID fragmentation.

Statistics

Data are presented as the mean ± S.E.M. in the *in vitro* study and the mean ± S.D. in the *in vivo* study. Statistical analyses were performed with Student's *t* test for the comparison of two groups or with the Tukey–Kramer test for the comparison of three groups. JMP 11 software (SAS Institute Inc., Cary, NC, USA) was used for statistical analyses. A two-tailed value of $p < 0.05$ was considered statistically significant.

Results

In Vitro Study

The radioactivity uptake of hypoxic cells was significantly higher than that of normoxic cells at 2 h after incubation with [18F]DiFA (hypoxia, 0.53 ± 0.02; normoxia, 0.26 ± 0.02 %dose/mg protein, $p < 0.01$; Fig. 2). The ratio of the radioactivity of the low-molecular-weight fraction was 66.3 ± 0.6% in the homogenates of the hypoxic cell (Fig. 2). As for [18F]FMISO, the radioactivity in the hypoxic cells was 0.34 ± 0.07 %dose/mg protein, which was significantly lower than that of the cells treated with [18F]DiFA in hypoxia ($p < 0.01$). The ratio of the radioactivity covalently bound to macromolecules was 27.1 ± 1.9% in the homogenates of the hypoxic cells treated with [18F]FMISO (Fig. 2).

In Vivo Distribution and Metabolism Study

The biodistributions of [18F]DiFA in FaDu-xenografted mice in each organ 1 and 2 h after administration are shown in Table 1. The tumor-to-blood (T/B) and tumor-to-muscle (T/M) ratios increased with time [T/B 0.84 ± 0.16 (1 h), 1.68 ± 0.36 (2 h); T/M 0.96 ± 0.18 (1 h), 2.18 ± 0.37 (2 h)].

The accumulation levels of [18F]DiFA in tumors were lower than those of [18F]FMISO (0.93 ± 0.19 *vs.* 4.87 ± 2.62 %ID/g at 2 h after administration), whereas the blood clearance was improved (0.56 ± 0.01 *vs.* 3.46 ± 1.14 %ID/g at 2 h after administration) (Fig. 3a). The T/B ratio was slightly higher for [18F]DiFA (1.68 ± 0.36 *vs.* 1.38 ± 0.42) (Fig. 3b). The partition ratios of the radioactivities in the low-molecular-weight fractions of the tumor homogenates were extremely high 2 h after the administration of [18F]DiFA or [18F]FMISO (90.4 ± 0.9% for [18F]DiFA, 88.4 ± 3.5% for [18F]FMISO) (Fig. 3c).

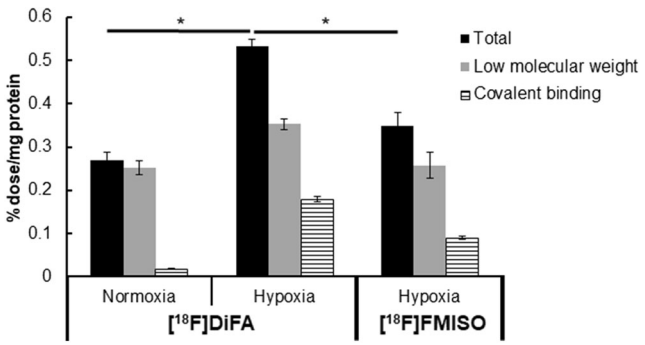

Fig. 2. Cellular uptake and metabolism of [18F]DiFA at 2 h post-incubation with tumor cells *in vitro* under normoxic and hypoxic (1% O_2) conditions. [18F]FMISO was also tested using tumor cells under hypoxic condition. Black bar, total radioactivity of cells; gray bar, radioactivity of the low-molecular-weight fraction of the cell homogenates; striped bar, radioactivity of the covalent binding to macromolecule fraction of the cell homogenates, *$p < 0.01$.

Table 1. Distribution of [18F]DiFA in FaDu-bearing Balb/c-nu mice at 1 or 2 h after administration. The results are expressed as %ID/g (mean ± S.D.)

	1 h	2 h
Blood	2.40 ± 0.89	0.56 ± 0.10
Heart	2.38 ± 0.96	0.54 ± 0.02
Liver	3.70 ± 1.29	1.01 ± 0.21
Kidney	6.54 ± 3.15	1.95 ± 0.33
Muscle	2.10 ± 0.81	0.43 ± 0.02
Bone	1.39 ± 0.40	0.39 ± 0.10
Tumor	1.97 ± 0.76	0.93 ± 0.19
Tumor/muscle	0.96 ± 0.18	2.18 ± 0.37
Tumor/blood	0.84 ± 0.16	1.68 ± 0.36

Distribution of DiFA and Its Derivative in Tumor Tissue Sections

The distribution of DiFA (*m/z* 234.088, $[M+H]^+$) in tumor tissue sections was visualized by MADLI-IMS analysis (Fig. 4b) and was found not to correspond to the distribution of radioactivities detected by an ARG study (Fig. 4c) and the positively stained areas of pimonidazole IHC staining (Fig. 4d). On the other hand, the distribution pattern of the unknown molecule with *m/z* 509.185 ($[M+H]^+$) (Fig. 4a) was similar to that of the radioactivity in the ARG images and the positively stained areas of pimonidazole IHC staining.

Identification of the DiFA Metabolite in Tumors

The isotope pattern of the molecule with *m/z* 509.182 ($[M+H]^+$) on tumor tissue sections was measured by ultrahigh resolution mass spectrometry (FT-ICR MS) and was found to correspond to that of the authentic amino-DiFA-GS and the theoretically calculated isotope pattern of amino-DiFA-GS (Fig. S1). From this result, the molecule with *m/z* 509.182 ($[M+H]^+$) on tumor tissues has the same chemical formula ($C_{18}H_{29}FN_6O_8S$) with amino-DiFA-GS. The chemical structure of the molecule with *m/z* 509.182 ($[M+H]^+$) was also analyzed by tandem mass spectrometry and showed fragmentation patterns similar to those of the synthesized amino-DiFA-GS (Fig. S2).

Discussion

In this work, we first evaluated whether [18F]DiFA really accumulated in hypoxic cells by an *in vitro* cellular uptake study. The radioactivity of [18F]DiFA-treated hypoxic cells was significantly higher than that of [18F]DiFA-treated normoxic cells, which suggests that [18F]DiFA can accumulate specifically in hypoxic cells, as we expected (Fig. 2). In addition, in comparison with [18F]FMISO, a well-used PET imaging probe for the diagnosis of hypoxia, [18F]DiFA showed significantly higher accumulation in the hypoxic cells (0.53 ± 0.02 *vs.* 0.35 ± 0.03%dose/mg protein, $p < 0.01$). These results suggest that [18F]DiFA has appropriate property as a hypoxia-targeting

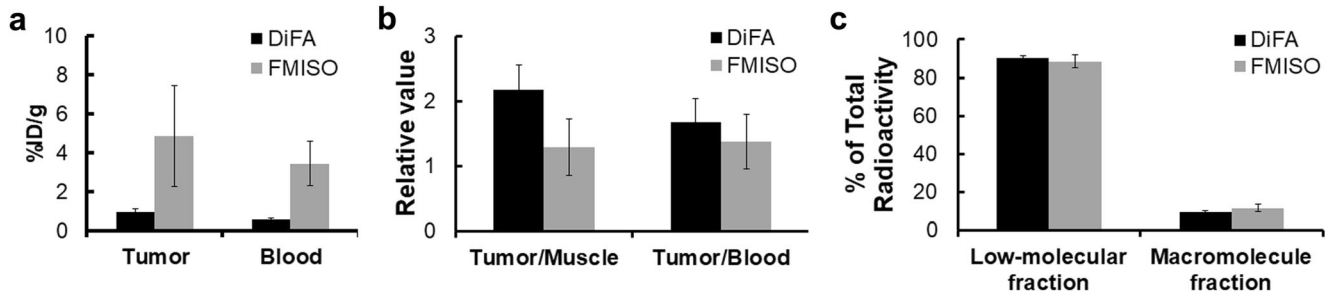

Fig. 3. **a** Radioactivity (%ID/g) of the tumor to blood at 2 h after administration of [^{18}F]DiFA (black) or [^{18}F]FMISO (gray). **b** Tumor-to-muscle or tumor-to-blood ratio at 2 h after administration of [^{18}F]DiFA (black) or [^{18}F]FMISO (gray). **c** Percentage of low-molecular-weight fraction or macromolecule fraction in the total radioactivity of the tumor homogenates at 2 h after administration of [^{18}F]DiFA (black) or [^{18}F]FMISO (gray).

probe. We also found that more than half of [^{18}F]DiFA accumulating in the hypoxic cells existed in the low-molecular-weight fraction similarly to [^{18}F]FMISO (Fig. 2). From this result, it is presumed that [^{18}F]DiFA is retained in the hypoxic cells by a metabolic process similar to that of [^{18}F]FMISO, which is metabolized mainly to be low-molecular-weight metabolites [13].

In the *in vivo* study, in addition to the biodistribution of [^{18}F]DiFA (Fig. 3a, b, Table 1), we also evaluated the partition ratios of the radioactivities in the low-molecular-weight fractions or covalently binding to the macromolecule fraction of the tumor homogenates and found that almost 90% of the radioactivity in the tumor homogenates existed in the low-molecular-weight fractions, whose value was closely similar to that of [^{18}F]FMISO (90.4 ± 0.9% for [^{18}F]DiFA, 88.4 ± 3.5% for [^{18}F]FMISO at 2 h after administration) (Fig. 3c). This result would support the notion that [^{18}F]DiFA undergoes a metabolic process similar to that of [^{18}F]FMISO as we observed in the *in vitro* study. The distribution of [^{18}F]DiFA in tumor tissue of our FaDu model was similar to the pimonidazole positively staining area. It is reported that pimonidazole distribution detected by IHC was heterogeneous and its binding (staining) level correlated highly with the hypoxic fraction in tumor tissues, which suggests that pimonidazole immunohistochemistry presents the hypoxic region in tissues [15]. Considering the results of

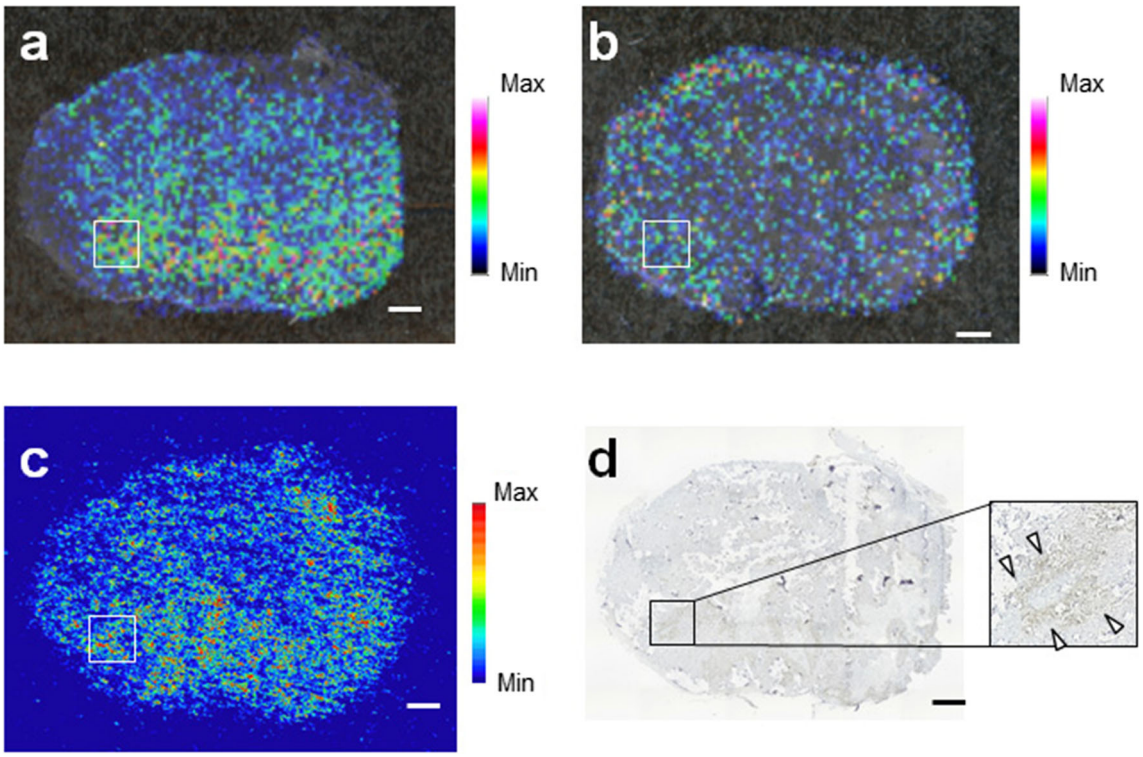

Fig. 4. **a** Representative mass spectrometric images of *m/z* 509.182 ([M+H]$^+$) representing amino-DiFA-GS and **b***m/z* 234.088 ([M+H]$^+$) representing DiFA. **c** ARG and **d** pimonidazole staining in FaDu tumor at 2 h after administration of [^{18}F]DiFA. Scale bar represents 1 mm.

the *in vitro* study and *ex vivo* comparison of ARG and pimonidazole IHC, [18F]DiFA would be distributed in the hypoxic region of tumor tissues.

Therefore, we next evaluated the metabolic process of [18F]DiFA in the hypoxic cells. To perform this evaluation, we used a combination of IMS and radioisotope analysis, since nuclear imaging techniques can provide only the distribution of the radioisotope but no chemical information. In the past few decades, IMS was developed as a novel imaging technique that allows the direct high-resolution visualization of the distribution of molecules in tissue sections [16]. Although it is quite difficult to acquire *in vivo* images, IMS has been used to investigate the distribution of a wide variety of molecules, not only endogenous biomolecules such as peptides and lipids, but also drugs and their metabolites [17–20]. Furthermore, IMS can visualize the distribution patterns of multiple molecules in a single measurement without any specialized probes, owing to the mass spectrometric detection technique [16]. This characteristic makes it possible to evaluate the distribution of specific drug-derived metabolites. To date, we have studied the accumulation mechanism of [18F]FMISO in hypoxic regions in tumor tissues by using a combination of IMS and radioisotope analysis. We found that the glutathione conjugate of reduced FMISO (amino-FMISO-GS) was the major metabolite involved in the hypoxia-specific accumulation [12, 13], in contrast to the conventional view that FMISO incorporation was mainly through the covalent binding to macromolecules [21]. This phenomenon was also observed in the other 2-nitroimidazole-based agent pimonidazole [14]. Thus, we assumed that [18F]DiFA was also metabolized to be a glutathione conjugate of its reduced form, similarly to [18F]FMISO. To test this hypothesis, we performed mass spectrometric analysis, especially IMS evaluation of tumor tissue sections derived from DiFA-treated mice. As we assumed, the mass signal with *m/z* 509.182 ($[M+H]^+$) was observed on the DiFA-treated tumor tissues, whose value coincides with the exact mass value of amino-DiFA-GS. The ultrahigh resolution mass spectrometric analysis revealed that the isotope pattern of this molecule corresponded to that of the amino-DiFA-GS that we synthesized and the calculated isotope pattern. This result indicates that the molecule with *m/z* 509.182 ($[M+H]^+$) observed on the tissue section had the chemical formula ($C_{18}H_{29}FN_6O_8S$) of amino-DiFA-GS (Fig. S1). Thus, we measured the molecule with *m/z* 509.182 ($[M+H]^+$) by tandem mass spectrometry and found that the fragmentation pattern of the molecule on tumor tissue sections was very similar to that of the synthetic preparation of amino-DiFA-GS (Fig. S2). This result suggests that the molecule with *m/z* 509.182 ($[M+H]^+$) on tumor tissue sections had the same chemical structure as amino-DiFA-GS. Therefore, we next evaluated the distribution of amino-DiFA-GS in the tumor tissue sections by IMS. The distribution pattern of amino-DiFA-GS resembled that of the radioactivity detected by ARG and the positively stained area of pimonidazole immunohistochemistry (a hypoxia immunohistochemistry) at 2 h after the administration of [18F]DiFA (Fig. 4). On the other hand, non-metabolized DiFA showed a homogeneous distribution pattern unlike the distribution of radioactivity and the pimonidazole-positive area (Fig. 4b), and other reductive metabolites of DiFA were not detected (data not shown). This phenomenon was also observed on the tumor tissue sections dissected at 1 h after the administration of [18F]DiFA (Fig. S3). These results suggest that DiFA was metabolized to be a glutathione conjugate in the hypoxic region of tumor tissues at the early phase of its administration as seen in our previous study with [18F]FMISO [13]. This outcome is matched with our previous study with

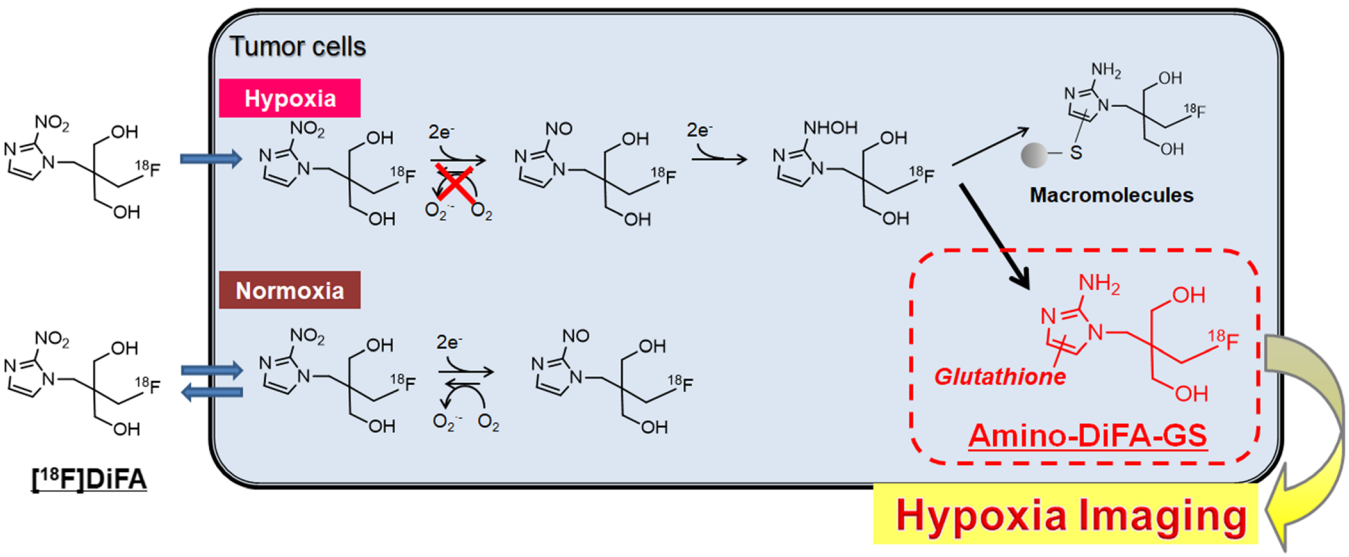

Fig. 5. Accumulation mechanism of [18F]DiFA in hypoxic cells suggested by this study.

pimonidazole, where the metabolism of a 2-nitroimidazole-based agent being a glutathione conjugate of the reduced form occurred at 30 min after the administration of the agent [14]. To take those results into account, after being taken up into hypoxic cells, [18F]DiFA would undergo glutathione conjugation reaction following reductive metabolism in hypoxic cells (Fig. 5).

While [18F]DiFA was highly taken up in the hypoxic cells compared to [18F]FMISO (Fig. 2), [18F]DiFA showed lower accumulation in the tumor tissue than [18F]FMISO in the *in vivo* study (Fig. 3). This discrepancy might be due to the rapid clearance of [18F]DiFA from the blood ([18F]DiFA 0.56 ± 0.01 *vs.* [18F]FMISO 3.46 ± 1.14 %ID/g at 2 h after administration) (Fig. 3a). The tumor-to-blood and the tumor-to-muscle ratios of [18F]DiFA-administered mice was slightly higher compared with those of [18F]FMISO-administered mice (tumor-to-blood ratio 1.68 ± 0.36 ([18F]DiFA) *vs.* 1.38 ± 0.42 ([18F]FMISO), tumor-to-muscle ratio 2.18 ± 0.37 ([18F]DiFA) *vs.* 1.29 ± 0.43 ([18F]FMISO) at 2 h after administration) (Fig. 3b), which would suggest that the distribution of [18F]DiFA was similar or relatively higher specificity to the hypoxic region of tumor tissues compared to that of [18F]FMISO. To take those results into account, the non-specific accumulation of [18F]DiFA would be disappear quickly from the tumor tissue.

Recently, we have reported that the accumulation level of [18F]FMISO in hypoxic cells was dependent on the cell type as well as the degree of the hypoxic state. This phenomenon was presumed to be affected by complicated cellular factors such as the cellular reduced glutathione (GSH) level and the expression levels and activities of glutathione S-transferases (GSTs), which catalyze glutathione conjugation reactions, and the multidrug resistant protein 1 (MRP1), which is one of the members of the ATP-binding cassette (ABC) transporter family and exports various kinds of glutathione conjugates out of cells [12]. The abilities of these cellular factors are known to be changed by not only tumor cell types but also cancer therapy [22]. For instance, it is reported that the GSH in tumor tissues is depleted by the treatment with anti-cancer drugs such as cisplatin, which is known to form glutathione conjugates in cancer cells in the process of detoxification [23]. Since this study suggests that [18F]DiFA undergoes the same metabolic pathway of [18F]FMISO in hypoxic cells, the distribution of [18F]DiFA in tumor tissues might be affected by cell type and cancer therapy. Therefore, further study is now under way to evaluate whether the factors mentioned above really influence the hypoxia PET imaging of [18F]DiFA.

Conclusions

In this study, we first showed that [18F]DiFA accumulated in cells depending on the hypoxic state. We then revealed that the glutathione-conjugated reductive metabolites of DiFA (amino-DiFA-GS) existed in the hypoxic regions of tumor tissues, as well as [18F]FMISO, within our FaDu tumor model. These results suggest that [18F]DiFA undergoes the glutathione conjugation reaction following reductive metabolism in hypoxic cells, which leads hypoxia-specific PET imaging with [18F]DiFA.

Acknowledgments. We thank the staff of the Hokkaido University Hospital Cyclotron Facility for the synthesis of [18F]DiFA and Reimi Kishi for her skillful technical assistance.

Funding Information This study was supported by the Acceleration Transformative Research for Medical Innovation program (ACT-M) from the Japan Agency for Medical Research and Development (AMED).

Compliance with Ethical Standards. The protocols for the experiments with tumor xenograft model mice were approved by the Laboratory Animal Care and Use Committee of Hokkaido University. The animal experiments were performed in accordance with the Guidelines for Animal Experiments of the Graduate School of Medicine, Hokkaido University.

Conflict of Interest

T. S., N. T., and Y. K. have grant support from Nihon Medi-Physics Co., Ltd. H. M is an employee of Nihon Medi-Physics Co., Ltd. The other authors declare that there is no conflict of interest associated with this manuscript.

References

1. Wilson WR, Hay MP (2011) Targeting hypoxia in cancer therapy. Nat Rev Cancer 11:393–410
2. Horsman MR, Mortensen LS, Petersen JB, Busk M, Overgaard J (2012) Imaging hypoxia to improve radiotherapy outcome. Nat Rev Clin Oncol 9:674–687
3. Weissleder R, Pittet MJ (2008) Imaging in the era of molecular oncology. Nature 452:580–589
4. Tamaki N, Hirata K (2016) Tumor hypoxia: a new PET imaging biomarker in clinical oncology. Int J Clin Oncol 21:619–625
5. Lopci E, Grassi I, Chiti A, Nanni C, Cicoria G, Toschi L, Fonti C, Lodi F, Mattioli S, Fanti S (2014) PET radiopharmaceuticals for imaging of tumor hypoxia: a review of the evidence. Am J Nucl Med Mol Imaging 4:365–384
6. Peeters SG, Zegers CM, Yaromina A, van Elmpt W, Dubois L, Lambin P (2015) Current preclinical and clinical applications of hypoxia PET imaging using 2-nitroimidazoles. Q J Nucl Med Mol Imaging 59:39–57
7. Troost EG, Laverman P, Philippens ME et al (2008) Correlation of [18F]FMISO autoradiography and pimonidazole [corrected] immunohistochemistry in human head and neck carcinoma xenografts. Eur J Nucl Med Mol Imaging 35:1803–1811
8. Toyonaga T, Hirata K, Shiga T, Nagara T (2017) Players of 'hypoxia orchestra'—what is the role of FMISO? Eur J Nucl Med Mol Imaging 44:1679–1681
9. Biskupiak JE, Krohn KA (1993) Second generation hypoxia imaging agents. J Nucl Med 34:411–413
10. Okamoto S, Shiga T, Yasuda K, Ito YM, Magota K, Kasai K, Kuge Y, Shirato H, Tamaki N (2013) High reproducibility of tumor hypoxia evaluated by ^{18}F-fluoromisonidazole PET for head and neck cancer. J Nucl Med 54:201–207
11. Nakata N, Okumura Y, Nagata E et al (2012) Evaluation of a new PET hypoxia tracer, [18F] HIC101, in comparison with [18F] FMISO. J Nucl Med 53:1523
12. Masaki Y, Shimizu Y, Yoshioka T, Nishijima KI, Zhao S, Higashino K, Numata Y, Tamaki N, Kuge Y (2017) FMISO accumulation in tumor is dependent on glutathione conjugation capacity in addition to hypoxic state. Ann Nucl Med 31:596–604
13. Masaki Y, Shimizu Y, Yoshioka T, Tanaka Y, Nishijima KI, Zhao S, Higashino K, Sakamoto S, Numata Y, Yamaguchi Y, Tamaki N, Kuge Y (2015) The accumulation mechanism of the hypoxia imaging probe "FMISO" by imaging mass spectrometry: possible involvement of low-molecular metabolites. Sci Rep 5:16802

14. Masaki Y, Shimizu Y, Yoshioka T, Feng F, Zhao S, Higashino K, Numata Y, Kuge Y (2016) Imaging mass spectrometry revealed the accumulation characteristics of the 2-nitroimidazole-based agent "pimonidazole" in hypoxia. PLoS One 11:e0161639
15. Raleigh JA, Chou SC, Arteel GE, Horsman MR (1999) Comparisons among pimonidazole binding, oxygen electrode measurements, and radiation response in C3H mouse tumors. Radiat Res 151:580–589
16. Caprioli RM, Farmer TB, Gile J (1997) Molecular imaging of biological samples: localization of peptides and proteins using MALDI-TOF MS. Anal Chem 69:4751–4760
17. Gobey J, Cole M, Janiszewski J, Covey T, Chau T, Kovarik P, Corr J (2005) Characterization and performance of MALDI on a triple quadrupole mass spectrometer for analysis and quantification of small molecules. Anal Chem 77:5643–5654
18. Vaidyanathan S, Gaskell S, Goodacre R (2006) Matrix-suppressed laser desorption/ionisation mass spectrometry and its suitability for metabolome analyses. Rapid Commun Mass Spectrom 20:1192–1198
19. Sugimoto M, Shimizu Y, Yoshioka T, Wakabayashi M, Tanaka Y, Higashino K, Numata Y, Sakai S, Kihara A, Igarashi Y, Kuge Y (2015) Histological analyses by matrix-assisted laser desorption/ionization-imaging mass spectrometry reveal differential localization of sphingomyelin molecular species regulated by particular ceramide synthase in mouse brains. Biochim Biophys Acta 1851:1554–1565
20. Sugimoto M, Wakabayashi M, Shimizu Y, Yoshioka T, Higashino K, Numata Y, Okuda T, Zhao S, Sakai S, Igarashi Y, Kuge Y (2016) Imaging mass spectrometry reveals acyl-chain- and region-specific sphingolipid metabolism in the kidneys of sphingomyelin synthase 2-deficient mice. PLoS One 11:e0152191
21. Prekeges JL, Rasey JS, Grunbaum Z, Krohn KH (1991) Reduction of fluoromisonidazole, a new imaging agent for hypoxia. Biochem Pharmacol 42:2387–2395
22. Riddick DS, Lee C, Ramji S, Chinje EC, Cowen RL, Williams KJ, Patterson AV, Stratford IJ, Morrow CS, Townsend AJ, Jounaidi Y, Chen CS, Su T, Lu H, Schwartz PS, Waxman DJ (2005) Cancer chemotherapy and drug metabolism. Drug Metab Dispos 33:1083–1096
23. Komiya S, Gebhardt MC, Mangham DC, Inoue A (1998) Role of glutathione in cisplatin resistance in osteosarcoma cell lines. J Orthop Res 16:15–22